9th AUSTRALASIAN
FLUID MECHANICS CONFERENCE,
AUCKLAND, 8-12 DECEMBER 1986

Pressure and Drag on Surface-Mounted Rectangular Plates and Walls

J. D. HOLMES

CSIRO Division of Building Research, Highett, Victoria, Australia.

ABSTRACT

Measurements of mean and peak net pressures on walls of various aspect ratios immersed in a simulated atmospheric boundary layer are described.

For wind directions normal to the walls, little variation of mean or peak pressures with position on the wall occurs. However for oblique wind directions much higher mean and peak pressures are found near the windward free end. For the normal wind direction, a minimum total mean drag coefficient at an aspect ratio of 5 was found, in agreement with recent Japanese work.

INTRODUCTION

Despite the extensive testing in boundary layer wind tunnels of enclosed buildings and other structures over the last twenty years, basic information on fluctuating and peak wind loads on simple rectangular walls and hoardings, is still lacking. Model studies carried out by the Division of Building Research of CSIRO, recently, are an attempt to rectify this situation; a part of this work is described in this paper.

The effects of aspect ratio (width/height), wind direction and, free ends were investigated and are described in this paper.

REVIEW OF PREVIOUS WORK

Good and Joubert (1968), and Sakamoto and Arie (1983) described measurements on two-dimensional and finite width plates mounted in smooth wall turbulent boundary layers of various depths. Sakamoto and Arie found a minimum drag coefficient at an aspect ratio of 5.

Ranga Raju et al. (1976) described measurements on two-dimensional plates in turbulent boundary layers, and presented a graph of drag coefficient, based on friction velocity, as a function of Jensen Number, h/z_o, where h is the height of the plate, and z_o is the roughness length. This graph is reproduced in Figure 1 of this paper. The data points are obtained from many tests in smooth and rough wall boundary layers, with values of h/δ, where δ is the boundary layer thickness, varying from less than 0.05 to greater than unity.

The drag coefficient C_D^* based on the friction velocity, u*, can be related to the drag coefficient C_{Dh}, based on the mean velocity at the height of the plate, $\bar{u}_h$, for plates fully immersed in the region of the boundary layer in which the logarithmic mean velocity profile applies, by the following:

$$C_D^* = C_{Dh} \left[\frac{1}{k} \ln \left(\frac{h}{z_o}\right)\right]^2 \qquad (1)$$

where k is von Karman's constant.

Equation (1) with C_{Dh} equal to 1.1 is a good fit to the data of Ranga Raju et al. in the range of h/z_o from 40 to 1000. Thus for practical purposes the mean drag coefficient

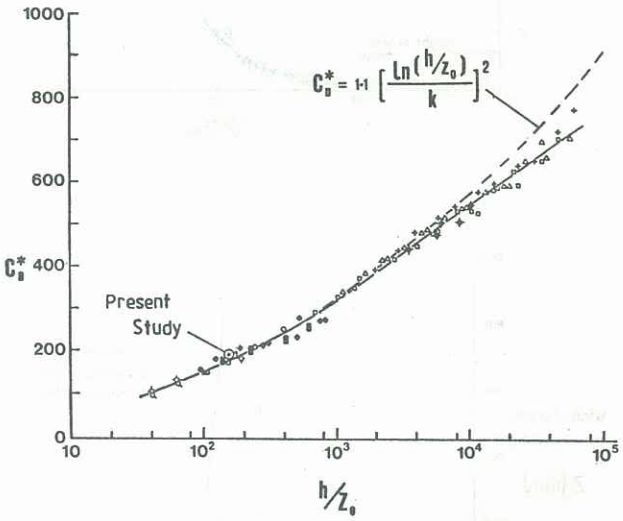

Fig. 1: Drag coefficients for two-dimensional walls in turbulent boundary layers (after Ranga Raju et al. (1976))

based on $\bar{u}_h$, is independent of the Jensen Number, over a large range of the latter.

EXPERIMENTAL TECHNIQUES

The present tests were carried out in the boundary layer section of the large low-speed wind tunnel at CSIRO Highett. The tunnel is of open circuit configuration with two right angled bends and two test sections, and is jointly operated by the Divisions of Building Research and Energy Technology. The boundary layer section has cross-section dimensions of 2 m (width) and 1 m (height), and a usable length of about 10 m.

A simulated strong wind atmospheric boundary layer flow was generated using the barrier/roughness technique described by Holmes and Osonphasop (1983). For the present study, a barrier of 250 mm height, with carpet roughness, designed to model flow over rural terrain was used. The barrier generates coherent eddy structures of a large scale, which are retained downwind well after the re-attachment of the shear layer shed from the barrier. Thus turbulence length scales appropriate to a scaled atmospheric boundary layer at a large geometric scaling ratio are generated.

Profiles of mean wind speed and longitudinal turbulence intensity measured at the centre of the wind tunnel turntable and two cross wind stations, 300 mm either side of the turntable centre, are shown in Figure 2. The centre of the turntable was 8.7 m downstream of the barrier - this is approximately twice the mean reattachment distance of the shear layer separating from the front of the barrier.

The profiles in Figure 2 are compared with the strong wind model profiles of Deaves and Harris (1978) for a geometric scaling ratio of 1/100, shear velocity, u_*, of 2 m/s and roughness length z_o of 40 mm. The latter is an appropriate

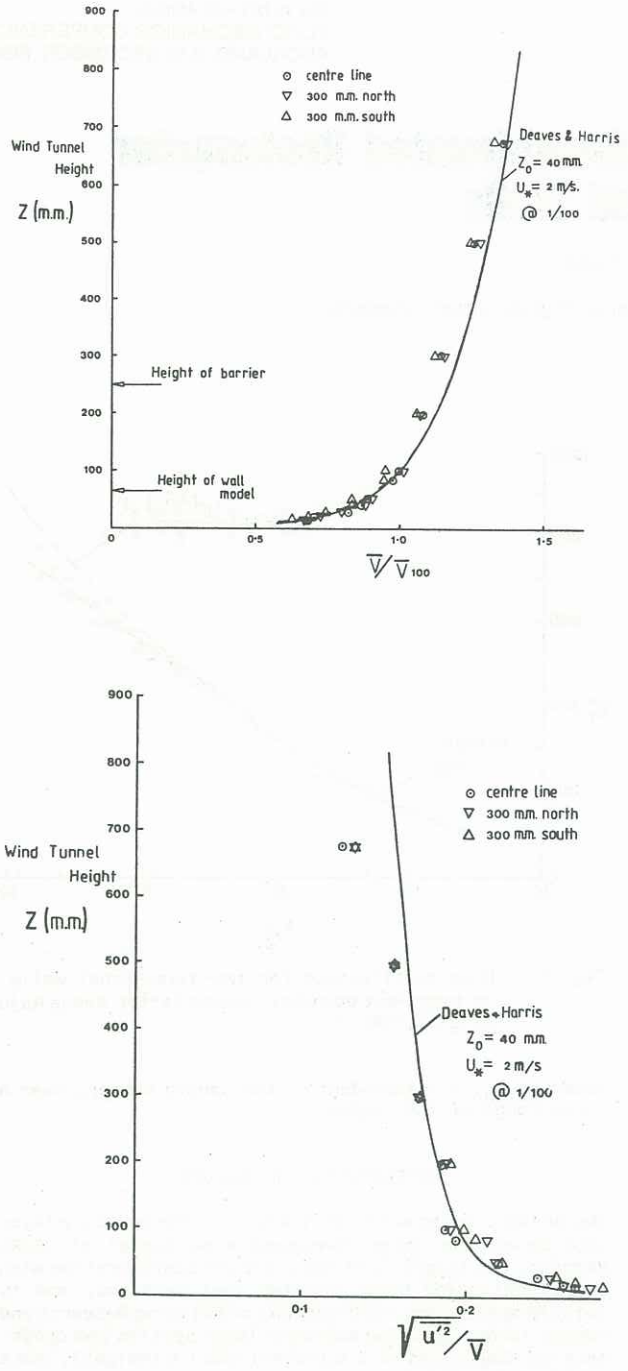

Fig. 2: Mean velocity (upper) and turbulence intensity (lower) profiles

value for rural terrain. Near the surface, the Deaves and Harris profiles are closely approximated by:

$$\frac{\bar{v}}{\bar{v}_{100}} = \frac{\ln (z/z_o)}{\ln (100/z_o)} \qquad (z_o \text{ in mm}) \qquad (2)$$

and

$$\frac{\sqrt{\overline{u'^2}}}{\bar{v}} = 0.094 + \frac{0.566}{\ln (z/z_o)} \qquad (3)$$

The longitudinal turbulence scale at a height of 100 mm in the wind tunnel, as determined from the longitudinal turbulence spectrum is approximately 400 mm - or 40 m at a height of 10 m in full scale. This is about half that quoted by E.S.D.U. (1974) for terrain of this type.

A rectangular plate of dimensions 64 mm height by 96 mm width by 4 mm thick, representing a section of a full-scale wall of 6.4 m height, was instrumented with pressure taps and transmission channels machined within the outer layers of the 'sandwich' construction. A total of 48 pressure taps - 24 on each side were provided. The pressure taps were internally manifolded in groups of six, forming a total of eight separate 'panels' - four on each side. Each panel was connected via p.v.c. tubing with short lengths of small diameter capillary tubing, to damp resonant peaks, inserted in the line to a Honeywell 163 pressure transducer so that simultaneous fluctuating pressure measurements were possible.

Each pressure measurement system, including pressure taps, channels, tubing, restrictors and transducers was separately calibrated using the apparatus described by Holmes and Lewis (1986). The restrictors were adjusted to give a flat amplitude frequency response to about 200 Hz. The phase responses were close to linear to 200 Hz and matched for the eight panels.

The panel pressures across the wall were subtracted to give sample records of the fluctuating normal force on sections of the plate. In this way, peak and r.m.s. net pressure differences, as well as mean values could be determined.

The mean wind speed at the height of the plate during the tests was 6.5 m/s giving a Reynolds Number based on t e wall height of 2.9×10^4. More significant for the present tests is the Jensen Number, h/z_o, which was about 160.

To represent walls of various aspect ratios, the plate was mounted on its own (aspect ratio, 1.5) and with non-instrumented side pieces to form walls of aspect ratios of 5, 10 and approaching infinity. In the latter case, the wall completely spanned the 2 m wide wind tunnel section or half the width for the semi-infinite case. Side pieces of various lengths were used to enable the loads at all sections of the long walls to be obtained.

The output of the pressure transducers were sampled by the A-D converters on a DEC 11/44 mini-computer system at a rate of 1000 Hz. Data processing was carried out on the 11/44 using a commercial software package. Several repeated readings of mean, r.m.s. and peak pressures for sample times of 23 seconds were taken. For the nominal length and velocity scales of the tests, this corresponded to about 10 minutes in full scale.

RESULTS

The results in this paper are all net pressure difference coefficients based on the mean wind speed at the height of the model in the wind tunnel (64 mm). During the pressure tests the mean dynamic pressure recorded by a pitot-static tube was used to compute the pressure coefficients. In a later test the ratio between this pressure and the dynamic pressure, based on the mean velocity at the model height at the centre of the turntable with the model removed, was accurately determined using a linearized hot-wire anemometer.

Blockage corrections were made using the values based on those suggested by McKeon and Melbourne (1971). The increment, ΔC_p, in the net wall pressure coefficient as a ratio of the corrected pressure coefficient C_{pt} is given by:

$$\frac{\Delta C_p}{C_{pt}} = 1.6 \frac{S}{A} \qquad (4)$$

where S is the projected area of the wall normal to the flow and A is the cross-sectional area of the wind tunnel.

Figures 3 and 4 show the mean pressure coefficients for walls of various aspect ratios for two different wind directions. Also shown are the average net pressure coefficients for the complete wall i.e. the force coefficient $\bar{C}_{Fx}$ based on the wall area. In the case of the normal wind direction in Figure 3, this is also the mean drag coefficient for the complete wall. For the small sections of wall where no direct measurements were taken,

an average from the adjacent panels was assumed for these calculations.

Figures 5 and 6 show the instantaneous peak pressure coefficients for the same two wind directions. These values were averages over at least four repeated runs, and for the higher pressures, many more runs than this.

DISCUSSION

The mean panel pressure coefficients for the wind direction normal to the plane of the plate (Figure 3) show relatively little variation with position of the panel on the plate, although there is a tendency for the pressures to increase towards the free ends of the plates of finite aspect ratio. The value of total drag coefficient of 1.16 for the two dimensional plate agrees well with the value of 1.15 found by Good and Joubert (1968), and with the composite curve of Ranga Raju et al. (1976) in Figure 1. A minimum mean drag coefficient is found at an aspect ratio of 5, in agreement with the result of Sakomuto and Arie (1983).

For the wind direction at 45° to the plane of the wall (Figure 4), very high mean pressure coefficients greater than 2 are found near the free ends of the longer aspect ratio walls. These are primarily caused by very high suctions on the rear face of the wall in this region, accompanying the strong shedding of vorticity with the shear layer from the front of the wall.

The peak pressure coefficients on the walls in Figures 5 and 6 reflect closely the characteristics of the mean pressures in Figures 3 and 4 suggesting that the pressure fluctuations are strongly related to the upwind turbulence in a quasi-steady way. However, the gust factors for the pressures, i.e. C_p/C_p, tend to reduce with increasing aspect ratio. This is due to the increasing distortion imparted on the turbulent flow as the aspect ratio increases (e.g. Bearman (1972), Hunt (1973), Holmes (1976)), and the attenuation of the pressure fluctuations on the rear face of the walls.

The measurements at CSIRO have been carried out in parallel with similar studies at Oxford University, Letchford (1985). The results show excellent agreement but because of space limitations, a comparison of the two sets of results will be deferred to another publication.

CONCLUSIONS

i) The net mean pressures on walls of various aspect ratios with winds normal to their planes, show little variation with position on the wall.
ii) Extremely high net pressures occur near the free ends of walls of finite aspect ratio for winds that are at 45° to the plane of the wall.
iii) A previous discovery of a minimum drag coefficient for an aspect ratio around 5 has been confirmed.
iv) The peak pressures on the walls show lower gust factors with increasing aspect ratio, demonstrating the effect of increasing distortion of the approaching turbulent flow.

REFERENCES

Bearman, P W (1972): Some measurements of the distortion of turbulence approaching a two-dimensional bluff body. J. Fluid Mech., Vol. 53, 451-467.

Deaves, D M; Harris, R I (1978): A mathematical model of the structure of strong winds. Construction Industry Research and Information Association (U.K.). Report 76.

E.S.D.U. (1974): Characteristics of atmospheric turbulence near the ground - Part II: single point data for strong winds (neutral atmosphere). Engineering Sciences Data Unit (U.K.). Data Item 74031.

Good, M C; Joubert, P N (1968): The form drag of two-dimensional bluff-plates immersed in turbulent boundary layers. J. Fluid Mech., Vol. 31, 547-582.

Holmes, J D (1976): Pressure fluctuations on a large building and along-wind structural loading. J. Ind. Aerodyn., Vol. 1, 249-278.

Holmes, J D; Lewis, R E (1986): Optimization of dynamic-pressure measurement systems - I. Single point measurement. Submitted to J. Wind Engg. & Ind. Aerodyn.

Holmes, J D; Osonphasop, C (1983): Flow behind two-dimensional barriers on a roughened ground plane, and applications for atmospheric boundary layer modelling. Proc. 8th Australasian Fluid Mechanics Conference, Newcastle.

Hunt, J C R (1973): A theory of turbulent flow round two-dimensional bluff bodies. J. Fluid Mech., Vol. 61, 625-706.

Letchford, C W (1985): Wind loads on free-standing walls. Dept. of Engineering Science, Oxford University, Report OUEL 1599/85.

McKeon, R J; Melbourne, W H (1971): Wind tunnel blockage effects and drag on bluff bodies in a rough wall boundary layer. Proc. 3rd International Conference on Wind Effects on Buildings and Structures, Tokyo.

Ranga Raju, K G; Loeser, J; Plate, E J (1976): Velocity profiles and fence drag for a turbulent boundary layer along smooth and rough flat plates. J. Fluid Mech., Vol. 76, 383-399.

Sakamoto, H; Arie, J (1983): Flow around a normal plate of finite width immersed in a turbulent boundary layer. J. Fluids Engineering, Vol. 105, 98-104.

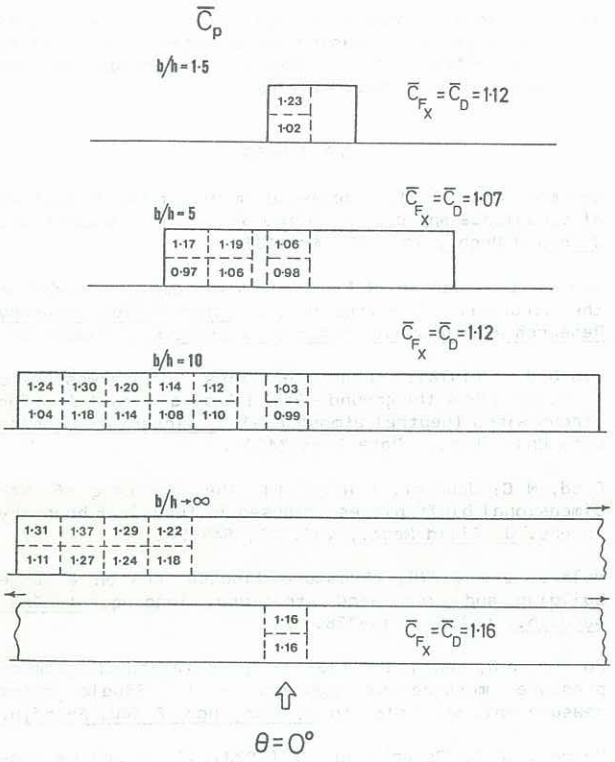

Fig. 3: Mean net pressures for normal wind

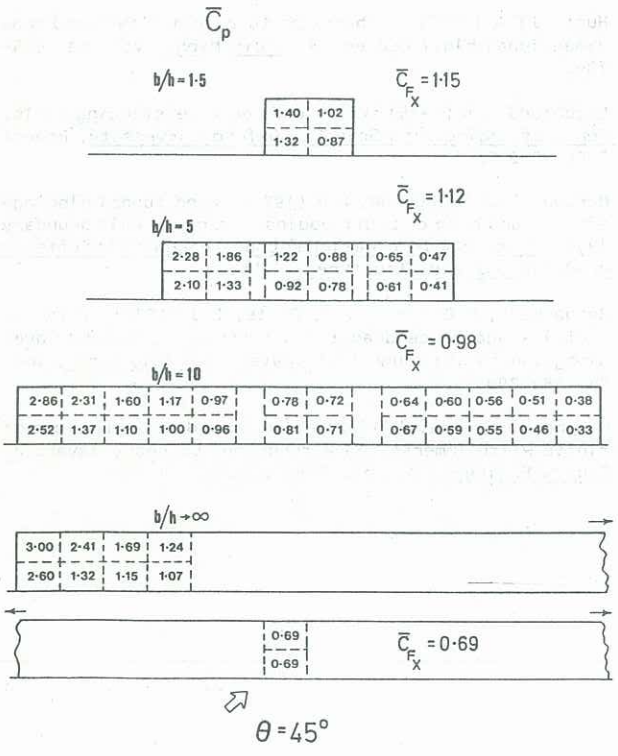

Fig. 4: Mean net pressures for oblique wind

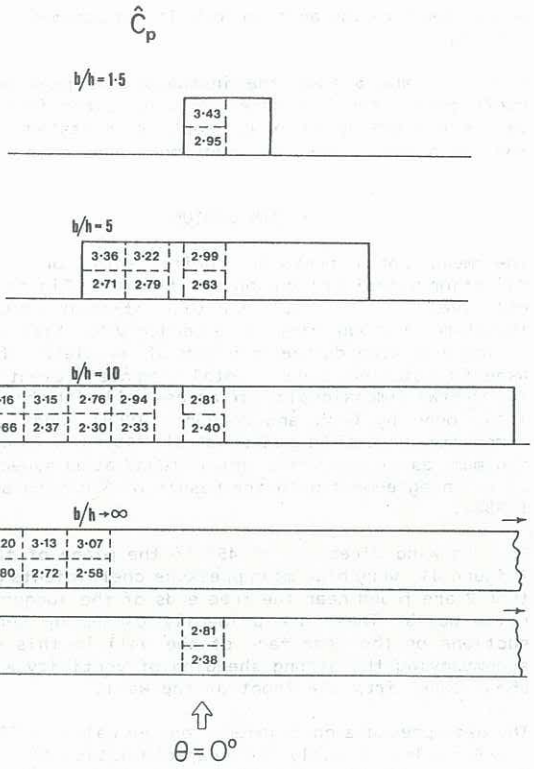

Fig. 5: Peak net pressures for normal winds

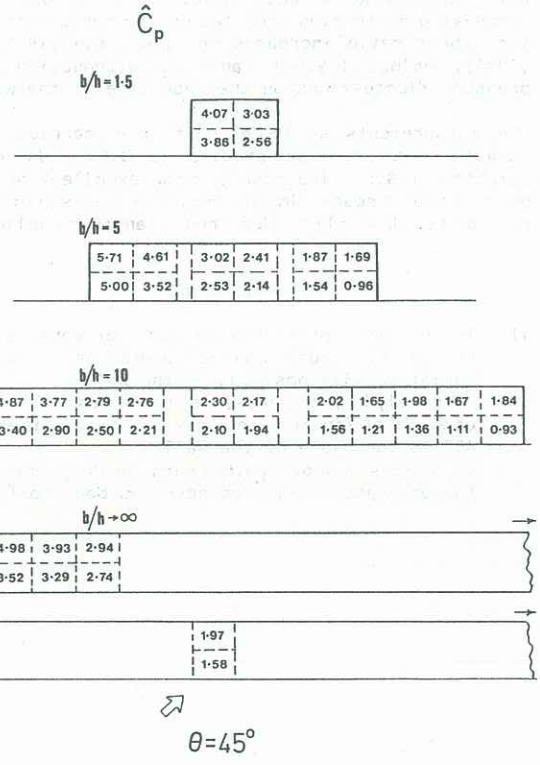

Fig. 6: Peak net pressures for oblique winds